Atomistic Processes in the Early Stages of Thin-Film Growth

Zhenyu Zhang and Max G. Lagally

Growth of thin films from atoms deposited from the gas phase is intrinsically a nonequilibrium phenomenon governed by a competition between kinetics and thermodynamics. Precise control of the growth and thus of the properties of deposited films becomes possible only after an understanding of this competition is achieved. Here, the atomic nature of the most important kinetic mechanisms of film growth is explored. These mechanisms include adatom diffusion on terraces, along steps, and around island corners; nucleation and dynamics of the stable nucleus; atom attachment to and detachment from terraces and islands; and interlayer mass transport. Ways to manipulate the growth kinetics in order to select a desired growth mode are briefly addressed.

The study of film growth has been increasingly characterized by the application of surface-science methods to understand growth at the atomic level. Work in this field has been motivated by the ever more stringent requirements on the quality of thin films needed for developing advanced microelectronic, optical, and magnetic devices, as well as the thrust toward nanometer-scale structures. As device miniaturization reaches submicrometer- and nanometer-length regimes, atomic-level control of the fabrication processes for both novel materials and new devices is becoming crucial.

A model study of film growth typically involves deposition of a controlled amount of atoms onto a well-characterized crystalline substrate at a prescribed set of growth conditions. The precisely defined growth conditions, low coverages, and slow deposition rates in such studies make it possible to decipher, at an atomic level, the rules governing the evolution of the growth front, and to explore ways to tailor film morphology to obtain specific characteristics.

Descriptions of atomistic mechanisms of growth have been largely based on the terrace-step-kink (TSK) model of a surface (Fig. 1) (*1*). In addition to defining steps, kinks, and terraces, Fig. 1 shows several elemental entities in film growth: an adsorbed atom (adatom) and a vacancy on the upper terrace, an adsorbed dimer (ad-dimer), and a larger island of four atoms in size. The scanning tunneling microscope (STM) (*2*) has allowed direct visualization of the TSK model (*3*). The STM can be used to determine quantitatively kinetic and thermodynamic properties of morphological entities on a surface as small as a single atom, as large as a micrometer-sized terrace, or as high as many atomic layers.

Information of this nature has allowed contact to be made with microscopic theories of film growth and has stimulated new theoretical developments. The synergism between experiment and theory has tremendously improved our understanding of the kinetic aspects of growth. For vapor-phase epitaxy, the film growth kinetics are largely determined by only a few categories of atomistic rate processes, which form the basis also for all more complex growth situations. We focus on these basic categories, illustrating them with examples from recent experiments. After describing the mechanisms, we suggest ways to manipulate them in order to select a desired growth mode. In more complex modes of growth, one or more additional mechanisms may influence the overall growth kinetics, although the mechanisms discussed here will of necessity still control the initial stages of growth. The brief discussion of such additional rate processes concluding this review recognizes their possible importance in general growth situations. A more comprehensive evaluation of such rate processes is beyond our scope, especially so as they are not yet well understood on the atomic scale. We focus on presenting physical ideas in a qualitative manner, rather than developing quantitative descriptions.

Adatom Diffusion on Terraces and Nucleation of Islands

The diffusion of an adatom on a flat surface, or terrace, is by far the most important kinetic process in film growth. Smooth, uniform films could not be formed without sufficient surface mobility. In the extreme case of zero mobility parallel to the surface, an adatom stays where it has landed, and the resulting growth front is always very rough. Nevertheless, higher surface mobility does not necessarily lead to smoother films.

The surface diffusion coefficient D is related to the site-to-site hopping rate of an adatom, k_s, by $D = a^2 k_s$, where a is the effective hopping distance between sites, and $k_s \propto exp\{-V_s/k_BT\}$, where V_s is the potential-energy barrier from site to site, T is the substrate temperature, and k_B is the Boltzmann constant. In the initial stage of growth on a flat surface, if the deposition rate F is fixed, the value of D determines the average distance an adatom will have to travel before (i) finding and joining an existing island or (ii) meeting another adatom to create the possibility of nucleating a new island. As nucleation continues, this distance decreases and eventually becomes constant. In this steady-state regime, newly deposited atoms will predominantly join existing islands and effectively prevent nucleation of new islands. Intuitively, the island density N should increase with F and decrease with D and has the qualitative form $N \propto F^p/D^q$ (*4*, *5*). The values of p and q are positive and are dependent on the nucleation and growth mechanisms.

Despite the vital importance of surface diffusion in film growth, accurate determination of D in a broad range of environ-

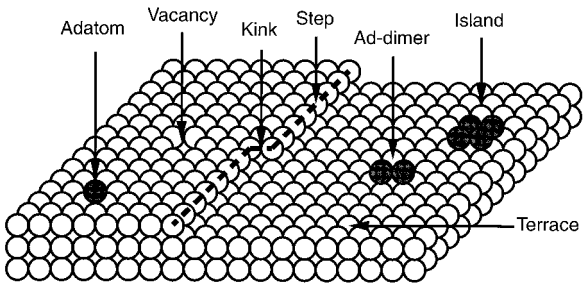

Fig. 1. The TSK model of a surface defined for a simple cubic crystal. The white circles represent atoms of the substrate. The dashed line indicates the location of a step separating the upper and the lower terraces, with a kink along the step. The step-down direction is from left to right. The black circles are atoms adsorbed on the terraces.

Z. Y. Zhang is a research staff member in the Solid State Division, Oak Ridge National Laboratory, Oak Ridge, TN 37831–6032, USA. E-mail: Zhangz@ornl.gov. M. G. Lagally is the E.W. Mueller Professor in the Departments of Materials Science and Engineering and Physics, University of Wisconsin, Madison, WI 53706, USA. E-mail: Lagally@engr.wisc.edu

ments has been a major challenge, but STM experiments have improved the situation considerably. The most prevalent approach (*5*) is based on nucleation theory (*4*): By counting the number of islands formed at a constant deposition flux and different temperatures, the diffusion coefficient can be extracted from the relation $N \propto D^{-q} \propto \exp\{V_s/qkT\}$, where the exponent q is known from nucleation theory once the critical island size is known. As an example (*5*), Fig. 2 shows silicon (Si) islands formed at two different temperatures on a reconstructed Si(100) (2 × 1) surface (*6*). This approach has been applied to a range of metal (*7*, *8*) and semiconductor (*9*, *10*) systems and has stimulated active research on generalizing classical nucleation theory (*4*) to various physically complicated situations (*11*–*13*).

A second approach (*14*, *15*) is to measure directly the mean square displacement, $\langle r^2 \rangle$, of a diffusing species as a function of time, t, and use the relation $\langle r^2 \rangle \sim Dt$ to obtain the diffusion coefficient, as has been done for many years with field ion microscopy (*16*, *17*). The potential advantage of STM is obvious, because STM can image a vastly broader range of surfaces than can field ion microscopy, whose applicability has been limited to primarily a few metals. A significant technical advance is the atom-tracking method, in which the STM tip automatically follows the position of an atom or a dimer as it migrates (*18*). Several other important recent developments (*5*, *19*, *20*) in surface diffusion will be addressed at relevant points.

Formation and Dynamics of the Stable Nucleus

As atoms join to form an island, the cohesive energy between the atoms acts to protect the island from dissociation, that is, the free energy of the island is negative. Atoms at the edges of the island have fewer neighbors, thus more unsaturated bonds, which add a positive destabilizing "boundary free energy" to the total free energy of the two-dimensional (2D) island. The boundary free energy is the 1D analog of the surface free energy. The latter is typically measured as the surface tension. In analogy, the boundary free energy can be considered as a line tension. For increasingly smaller islands, the boundary free energy dominates more and more, until an island is no longer stable against decomposition. Conversely, to nucleate an island, enough atoms have to meet to make the total island free energy negative, because initially the boundary free energy dominates and the total free energy becomes more positive as atoms are added. In nucleation theory, the "critical island size" i is defined as the size at which for the first time the island becomes more stable with the addition of just one more atom.

For a given system, i depends on temperature and supersaturation. Recent studies of submonolayer growth on semiconductor (*5*, *9*, *10*) and metal surfaces (*7*, *8*) have often suggested that, at sufficiently low temperatures, for typical growth conditions, the adatom supersaturation on the surface is so high that the critical nucleus is just a single atom, and the stable nucleus is two atoms, a dimer. These dimers then serve as the centers for growth of larger islands, as more adatoms diffuse to meet them.

Much recent attention (*21*–*26*) has been focused on the possible pathway for nucleation of a Si ad-dimer, the stable nucleus for a wide range of growth conditions for homoepitaxy on Si(100) (*5*). A Si adatom may have multiple diffusion pathways on the surface before finding a partner, as all calculations have suggested (*23*). Empirical-potential molecular dynamics simulations have suggested that in the earliest stages of adsorption, a Si atom deposited from the gas phase is more likely to be collected by a shallower local minimum within a unit cell, rather than landing directly in a stable adsorption site (*20*). Such a population inversion is possible because the energy transfer at that shallower site can be more effective, and because less kinetic energy has been accumulated by the atom in reaching this shallower site. If the potential-energy barrier for the adatom to reach a stable site is much higher than the barrier for it to reach another metastable site, then the adatom will travel a long distance along a path connecting the metastable sites before eventually reaching a stable site. Furthermore, whenever the adatom is able to hop out of a stable site, it can travel a long distance again before returning to another stable site (*23*).

Population inversion in the earliest stages of adsorption and fast-track diffusion is, in principle, possible whenever atoms are deposited on a complex reconstructed substrate. The validity of these qualitative conclusions should not depend on the specific potential used in the studies. For Si atoms on Si(100), fast diffusion on top of a dimer row is predicted by empirical-potential calculations (*20*, *23*). This same conclusion can also be inferred from the results of first-principles calculations (*23*–*26*). Although adatom motion has not been directly observed, it presumably leads to the nucleation of dimers, which occurs predominantly on top of dimer rows (*21*, *22*).

The stable nucleus, by definition unlikely to decompose, may not be stable in the sense of "stationary," but may have intriguing dynamical aspects, as has been demonstrated recently for Si dimers on Si(100) (*14*, *18*, *21*–*23*, *26*). Silicon dimers formed on top of dimer rows can have two orientations, with the dimer bond parallel or perpendicular to the substrate dimer rows. These two configurations are mutually convertible at room temperature through a rotational mode (Fig. 3). The active rotational motion helps to establish thermal equilibrium between the two configurations.

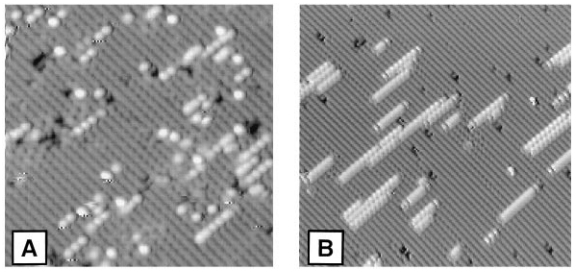

Fig. 2. STM images of monolayer-high Si islands on Si(100) grown with the same deposition rate and total coverage, but at different temperatures (*5*): (**A**) grown at low temperature, image size of 250 Å by 250 Å; and (**B**) grown at high temperature, image size of 400 Å by 400 Å. Brighter areas indicate atoms in a higher layer. Each bright row is made up of dimers, giving a (2 × 1) surface reconstruction. At both temperatures, the islands are oriented perpendicular to the substrate dimer rows. In (A), the slower adatom diffusion leads to a higher island density, including many isolated dimers. Some of the islands are "diluted," that is, every other dimer is missing along the long island direction. In (B), the islands are dense except that some have "diluted" ends. For a schematic representation of the 2 × 1 reconstruction of the surface resulting from dimerization of top-layer atoms, see Fig. 3.

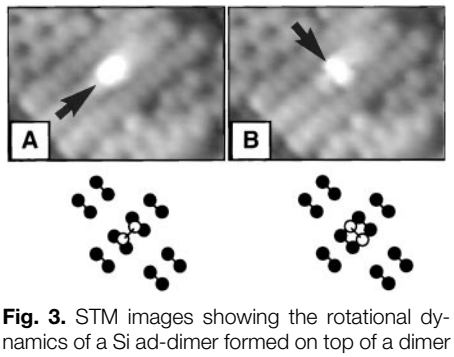

Fig. 3. STM images showing the rotational dynamics of a Si ad-dimer formed on top of a dimer row in Si(001) (*21*). In (**A**), the bond of the ad-dimer (indicated by the arrow) is parallel to the substrate dimer rows in the 2 × 1 reconstruction, as schematically shown below the image. In (**B**), the same ad-dimer has rotated by 90°. The two images were taken 40 s apart at room temperature. The orientation shown in (A) is energetically slightly more stable.

Simply by counting the population of these two states, their relative stability can be established (*21*). By measuring the rotational frequencies from one configuration to the other, the potential-energy barrier separating the two configurations can also be determined (*21, 26*). These measurements conclude that the "epitaxial orientation," the orientation of a dimer in the dimer rows that subsequently grow (Fig. 3A), is slightly more stable.

In addition to rotational motion, Si dimers located on top of a dimer row have been observed to diffuse along the top of the dimer row (*14, 18*), or, upon annealing, to jump into the trough defined between two neighboring dimer rows (*21*), suggesting that the trough is energetically more stable for a dimer. At present, this conclusion is controversial, because first-principles total-energy calculations have so far all come to the opposite conclusion (*23–26*). Alternative possibilities suggested for this apparent "jump" of the dimer into the troughs include stabilization by defects or by a third Si adatom (*25*). Although the mechanism is not precisely known, the ability to measure the influence of a single adatom on the behavior of a nucleus of two atoms indicates how far the understanding of nucleation and growth has come.

At higher surface coverages, islands grow from the stable dimers. As shown in Fig. 2B, particularly straight dimer-row islands with high shape anisotropy are formed at high temperatures (*5, 27*). The formation mechanisms involved are not yet fully understood (*20, 27*). These islands are not compact, but are dense except possibly at the two ends, with ad-dimers all epitaxially oriented and occupying all available sites, both those on top of and those between the dimer rows. At the ends of a dimer-row island, a dimer has frequently been observed one lattice site away from the proper end of the island. Such a "diluted-end" dimer has only been observed in one of the two possible positions, on top of a dimer row. Complete diluted-dimer islands, in which every other dimer is missing along the direction of the island elongation, have been observed for deposition near room temperature (*28*). Precisely how atoms attach to stable dimers to form those various islands (or larger islands in any other system) is unknown. The answer to this question will provide the missing link between nucleation and the subsequent growth of islands.

Similar STM studies of nucleation and growth have been carried out for metals (*8*). In these studies, it has not been possible to image entities as small as a dimer with sufficient resolution so that a dimer could be unequivocally identified. The average size of the smallest stable islands was inferred, instead, by counting the total number of islands at a given coverage. The critical island size, $i = 1$, was established by fitting the coverage dependence of the total island density with the standard classical nucleation model (*4*), in which i is a parameter.

Possible values for a critical island size greater than 1 depend on the specific bonding geometry of a given system (*13*) and, consequently, the relative magnitudes of the boundary free energy and the island cohesive energy. At sufficiently high temperatures, the critical island size may increase because thermal energy acts as an additional destabilizing factor. Critical sizes ranging from three atoms (*7*) to as high as ~650 dimers (*29*) have recently been reported. The latter case suggests that at typical realistic epitaxial film growth conditions of deposition rate and temperature, the surface is much closer to the thermodynamic than to the kinetic limit, that is, there is effectively no significant supersaturation.

Diffusion Along Island Edges and Fractal Island Growth

As islands continue to grow, specific island morphologies or shapes develop. One class of shapes—including squares, triangles, and hexagons—is compact, with relatively straight and equiaxed island edges. Another class is fractal-like, having rough island edges or highly anisotropic shapes (*30–32*). Typically, growth at lower substrate temperatures leads to less compact islands: The compactness is largely controlled by how fast an adatom diffuses along the island edges and crosses corners where two edges meet. Recent studies (*30–37*) of 2D island formation in metal-on-metal epitaxy have identified several aspects of atom diffusion along island edges that are important in controlling the formation of fractal islands.

In these studies, it has become evident that fractal island growth is very dependent on bonding geometry (*33*). The existence of fractal islands has been reported essentially only on face-centered-cubic (fcc) (111) or hexagonal close-packed (hcp) (0001) substrates, which both have approximate triangular lattice geometry. In contrast, growth on fcc(100) surfaces with square lattice geometry has so far always resulted in compact islands. This observation is in distinction to the prediction of the classic diffusion-limited-aggregation (DLA) model (*38*). Within this model, if a diffusing atom sticks to an island where it hits the island, then fractal islands will be formed, irrespective of lattice geometry. Furthermore, in the DLA model, the average branch thickness b of the fractal island is about one atom wide ($b \approx 1$), while the fractal islands observed with the STM all have wider branch thicknesses (*30–32, 35–37*).

These discrepancies can be accounted for by generalizing the hit-and-stick DLA model to situations more appropriate to real growth systems (*33*). In real growth, atoms are randomly and continuously deposited on the surface, and an adatom reaching an island will attempt to relax locally in order to find an energetically more favorable configuration. For a given system, the specific pathways available for such local relaxation depend on how the edge atom is bonded to the substrate and to the atoms already in the island. In terms of an increasing degree of local relaxation (such as increasing temperature), several different fractal-like growth regimes can be defined as follows:

Hit-and-stick DLA (regime I) (*33, 38*). Zero local relaxation defines this regime, characterized by $b \approx 1$. Its realization requires that an adatom arriving at the edge of an island does not have time to relax to a more favorable site before it is "pinned" in the position by the arrival of one or more additional atoms. To date, the formation of regime I fractals has not been observed in any film growth from vapor. The implication is that, at the growth conditions that have so far been studied, the relaxation to a more favorable site is always faster than the arrival rate to the same site [which depends on the deposition flux and the surface diffusion rate in a complicated manner (*33*)]. For metal (100) surfaces, this conclusion is not too surprising, because surface diffusion is generally hindered by the relatively large barriers between sites. If surface diffusion is slower than diffusion along steps, the existence of regime I fractal growth will be ruled out. This prohibitive condition is likely to be relaxed in those systems in which surface diffusion takes place through the place exchange mechanism (*19*), because the corresponding diffusional activation barriers can be much lower. For metal (111) surfaces for which surface diffusion is rapid, regime I fractal growth should be obtainable with higher deposition fluxes. It is possible, of course, that a local strain effect can destabilize onefold-coordinated sites.

Extended fractal growth (regime II) (*33*). In this regime, every adatom reaching the edge of an island can relax to the extent that it has found at least two nearest neighbors within the atoms belonging to the island. This regime can be defined on a triangular lattice, but is absent on a square lattice, for which this condition already implies compact islands (Fig. 4). Regime II fractal islands are characterized by having wider branch thickness, $b \approx 4$. Island morphologies in regimes I and II are contrasted in Fig. 5. For systems allowing the existence

of regime I fractal growth, regime II can be entered when an increase in surface temperature destabilizes those edge atoms that are only onefold coordinated. A measurement of the transition temperature from regime I to regime II provides an estimate of the potential-energy barrier, $V_e(1)$, hindering the relaxation of a onefold-coordinated edge atom.

Island-corner barrier effect (*34*). Even if the temperature is high enough to make possible adatom diffusion along island edges, it may still be difficult to cross the corner of an island at which two edges meet. The reason for this is that an adatom has to lower its coordination in crossing a corner. That it does not want to do so is reflected by a higher activation barrier as an atom leaves the edge to reach a corner site. Without direct or effective island corner crossing, growth must lead to the formation of fractal islands. The branch thickness of the islands in this regime increases with the rate of edge diffusion, that is, with the surface temperature: $b(T) > 4$. When b is sufficiently large, the growth of the fractal-like islands can also be described with quasi-continuum approaches (*11*, *39*). In such approaches, the fractal-to-compact transition is typically measured by an average diffusion length of an adatom along the island edge, with the assumption of an effective hopping rate. Such quasi-continuum approaches break down when the island branches are only one or a few atoms wide.

Although the absence, to date, of regime I fractal growth on any substrate may have its origin in the condition $V_e(1) < V_s$, the absence, to date, of any fractal growth on square lattices may be attributable to a similarity in barriers for diffusion across island corners and on terraces in such systems.

Compact islands. If all island corners can be crossed easily by an adatom, the growth leads to compact islands. On triangular and square lattices, the compact regime corresponds to relaxation to at least three and two nearest neighbors, respectively. On reconstructed surfaces, the situation may be more complex because of the complex bonding, but the principle for obtaining compactness, that is, the need to cross corners, will be universally applicable. In the compact-island growth regime, competition between steps of different orientations in accommodating arriving adatoms determines the shapes of the islands. Considerable effort (*31*, *40*) has been devoted to understanding the formation mechanisms of islands of various shapes, but many questions remain, particularly because in this regime many rate processes are active simultaneously.

In defining the four different regimes, attention has been focused primarily on in-plane interactions between the adatoms, implying that these interactions dominate the rules for island growth. The specific substrate geometry of a given system may introduce additional complications. For example, on fcc(111) surfaces, two structurally different types of steps exist (Fig. 6C), and diffusion along these two steps can be different (*31*). This difference in mobility along the two steps also introduces an asymmetric probability as a onefold-coordinated atom located at an island corner jumps toward more highly coordinated sites on either side of the corner (*36*). This corner asymmetry has been shown to provide a mechanism for dendritic (branched) island growth in several systems (*36*, *37*). Briefly, if both motions are possible but with different rates, onefold-coordinated atoms highly preferably fill the sites reachable along the easy path first. Dendritic islands with triangular envelopes develop on such fcc(111) surfaces. The corresponding branch thickness of the dendritic islands is about four atoms, as expected for islands grown within regime II. Furthermore, there is also a lower-temperature regime where only the easy path is active, leading to the formation of less well developed dendritic islands with $b \approx 2$ (*35*, *36*). As far as the branch thickness is concerned, these latter islands provide the closest example reported so far toward realization of the regime I fractals predicted by the classic DLA model, although their existence depends on an entirely different mechanism.

Although growth on semiconductors appears to be more complex because of reconstruction and localized bonding, in fact, simple analogies with the above picture exist (*34*). For example, the elongated dimer-wide islands (Fig. 2B) formed in Si(100) homoepitaxy can be viewed as a consequence of a morphological instability in low-temperature growth. Although the islands do not appear fractal-like, it is only the large anisotropy in diffusion and sticking that makes them long and narrow. This instability—growth takes place predominantly in one direction—is suppressed at higher temperatures, where the islands become compact as a result of island coarsening (*27*). Conceptually, these phenomena resemble very closely those described above for metal growth (*34*). The only major difference is the (fractal) dimension, d: in the special case of Si $d \sim 1$, while in the metals $d \sim 1.7$. The physical origin of this difference lies in the strong covalent bonding on the semiconductor surface.

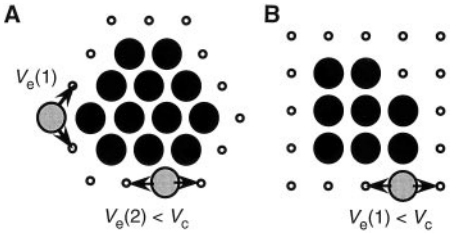

Fig. 4. Island formation on (**A**) a triangular and (**B**) a square lattice. The smaller open circles denote the sites accessible on each lattice. The larger circles denote atoms in the islands. The relaxation of an edge atom (gray) is hindered by the potential-energy barrier $V_e(1)$, when starting from a onefold-coordinated site (on both lattices), or by $V_e(2)$, when starting from a twofold-coordinated site (on the triangular lattice). On both lattices, it is easier for an atom to diffuse along an edge than to reach a corner site, because its coordination is always larger along the edge than at the corner.

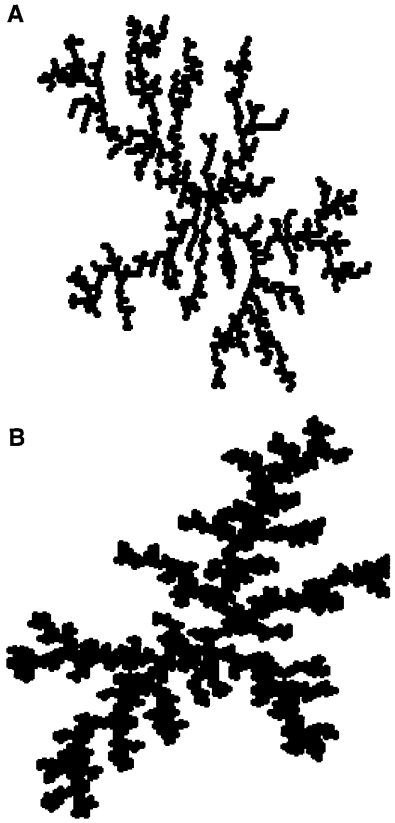

Fig. 5. Fractal islands grown on a triangular lattice in regime I (**A**), in which an atom sticks where it hits the island; and regime II (**B**), in which every atom is allowed to find at least two nearest neighbors of atoms belonging to the island (*33*). The branch thickness in regime I is about one atom and is four atoms in regime II.

Island Mobility and Ripening

The previous discussion has been confined to the temperature regime in which only the dynamics of those edge atoms that are severely undercoordinated are considered. The corresponding island dynamics are locally confined, with negligible displacement of the center of mass of the island. The driving force for evolution of the island

shape toward being compact is the minimization of the total free energy of each island, as edge atoms find more stable configurations.

As the surface temperature increases, atoms that were stable at lower temperatures (that is, with higher coordinations) can become active. Examples include evaporation of an atom from a step onto a terrace, ejection of an atom from a kink site, removal of a corner atom of an island, and the creation of an atom-vacancy pair along a step (*41*). These events lead to two new aspects of island dynamics: island diffusion and "ripening." Island diffusion is characterized by a finite displacement of the center of mass of an island. Ripening involves the redistribution of mass in an island and between different islands.

Island diffusion can proceed by many different mechanisms. In general, smaller islands diffuse faster than larger islands, but even very large adatom or vacancy islands can have significant mobility at room temperature (*42*). For sizes less than 10 atoms, oscillatory behavior of the island mobility with island size has been observed on metal surfaces (*43, 44*). The oscillatory behavior on fcc(100) metals (*44*) has been explained by invoking a combination of sequential motion of individual atoms and dimer shearing (*45*). The proposed kinetic mechanism is illustrated in Fig. 7 for a compact tetramer: diffusion of the island occurs by first shearing half of the island forward, followed by motion of the other half to catch up. Island shearing is more favorable than the atom-hopping process (Fig. 7B) because the former requires a lower activation energy. The energy gain becomes higher as the in-plane bonding strength between the adatoms increases, making the shearing process more favorable.

Ripening (*46*), a thermodynamically driven effort to reduce boundary free energy, occurs only if the net supersaturation of adatoms is very small. At conventional conditions for growth experiments, there is a high supersaturation so ripening is not important, as all islands larger than the critical size grow. However, the rate of ripening illustrates an important kinetic mechanism, the detachment rate of atoms from islands. In ripening, larger clusters grow at the expense of smaller ones. In film growth, the onset temperature for island ripening is about the same as for the fractal-to-compact island shape transformation (*34*). This recognition is tied to the island-corner barrier effect: without frequent corner crossing, islands will remain fractal-like. However, the very processes leading to the compaction of islands may also lead to the dissociation of smaller islands, because an atom crossing an island corner will have the highest probability of any atom to leave the island. Thus, "leaking" of atoms can occur preferably at island corners. Atom detachment directly from island edges occurs at higher temperatures (*34*).

Barrier for Crossing Steps

In film growth, the rate for interlayer mass transport is second only to surface diffusion in importance. Surface diffusion controls the uniformity in the horizontal direction; interlayer mass transport controls the uniformity in the vertical direction. A smooth growth front can be maintained only if sufficient interlayer mass transport occurs during growth.

Interlayer mass transport is primarily controlled by the barrier for crossing steps. An atom landing on top of an island may find a higher potential-energy barrier as it attempts to hop off the island to the lower layer. As in the case of island corner crossing for compact 2D growth, this additional barrier exists because an atom reduces its coordination as it crosses the island edge (*16, 47*). Therefore, it is more likely to be confined to the top of the island than to hop off, increasing the density of monomers there and thus the probability that a new island is nucleated on top of the existing island before growth of the first layer is completed (*48–51*).

The effect of the island-edge barrier on the film morphology has recently been broadly explored (*52–54*). If the effect is strong, 3D islands or "mounds" will develop and the growth mode is rough. If the effect is weak, the system can easily reach a stable growth regime with a smooth growth front. The strong regime of the island-edge barrier effect is separated from the weak regime by $R_c = R_{co}$, where R_c is the island size at which nucleation initiates on top of the island and R_{co} is the island size at which island coalescence in the lower layer initiates (*48*). If $R_c < R_{co}$, the island-edge barrier effect is strong enough to cause rough growth; otherwise the effect is weak, and the growth mode is smooth. For relatively small islands, a condition for suppressing 3D growth is provided by the requirement that an atom landing on top of an island is able to hop off before a second atom lands on top of the same island. A probability factor describing this condition has been derived, and ways to enhance this factor in order to induce layer-by-layer growth have been discussed (*50*).

Manipulation of Growth Kinetics

We have so far described the major categories of atomistic rate processes important in the initial stages of film growth: adatom diffusion on terraces, along steps, and around island corners; nucleation and dynamics of the stable nucleus; mechanisms for the addition of atoms to a growing island; mechanisms for the detachment of an atom from a structure; and interlayer mass transport. Explorations seeking improved understanding of the relative importance of

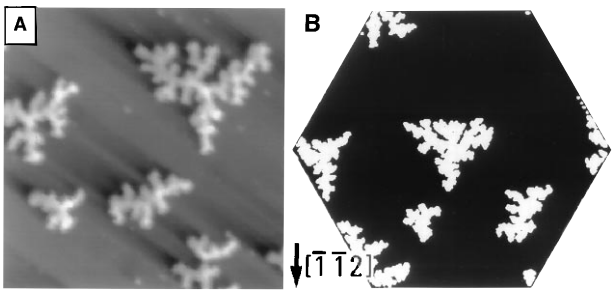

Fig. 6. STM images and corresponding simulations of dendritic Pt islands grown on Pt(111) (*36*). Shown are (**A**) an STM image, of 500 Å by 500 Å, and (**B**) island shapes obtained from kinetic Monte Carlo simulations. These dendritic islands have the same branch thickness as the regime II fractal island shown in Fig. 5B, but with triangular envelopes. This difference is caused by the corner asymmetry shown schematically in (**C**): if the sublayer symmetry of the fcc lattice is considered, the two edges are inequivalent, and a onefold-coordinated atom finds it easier to go to one edge as it relaxes [$V_{e,b}(1) < V_{e,t}(1)$]. The smaller open circles denote the fcc sites accessible to the adatoms.

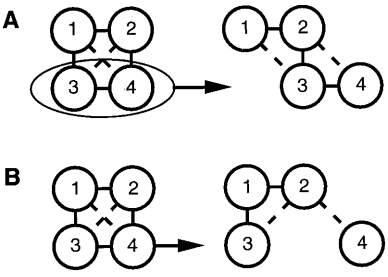

Fig. 7. Competing diffusion mechanisms of a compact tetramer island on a metal (100) surface. (**A**) Diffusion by dimer shearing proceeds by first placing half of the island forward, followed by the other half. (**B**) Diffusion by sequential motion of individual atoms. The (A) pathway can be the preferred mode of island motion under appropriate limits on bond strengths.

these processes have led to discoveries of various ways of rate manipulation to improve the quality of films grown by vapor-phase epitaxy (*48*–*53*, *55*, *56*). For example, any enhancement of downward diffusion would improve layer-by-layer or 2D growth. Any enhancement of corner crossing would lead to more compact islands. Any enhancement of surface diffusion would lead to earlier achievement of step-flow growth (see below). As an example, we list several suggestions for improved 2D homoepitaxial growth at low temperatures, that is, to enhance downward diffusion by making it easier to cross steps.

Reduction in the island-edge barrier. A direct reduction in the island-edge barrier, in principle, provides the most effective way to improve 2D growth.

Hindering diffusion along island edges by impurities. Slower diffusion along steps leads to a higher density of kinks in the island edges. Typically, an atom landing on top of such an island can hop down more easily at a kinked site than at a straight step (*52*), although the degree of enhancement depends on the specific local bonding geometry and the step-down mechanism (*57*).

Increase in island density (*51*). Two-dimensional growth can be enhanced if the islands in the first incomplete layer are small, because an atom on top of a smaller island will visit the island edges more frequently, thereby increasing its chance to hop down. An increased island density can be achieved in various ways, such as use of a surfactant (see below), simultaneous sputtering or etching of the surface during deposition, a nonuniform-temperature deposition scheme (a small dose at low temperature followed by the completion of the layer at higher temperature), or, equivalently, a nonuniform-flux deposition scheme (a small dose at high flux followed by the completion of the layer at lower flux).

Mobility bias. With all other conditions fixed, an enhancement in atom mobility on top of an island with respect to that on the lower layer will improve 2D growth because, again, an atop atom will more frequently reach the island edge and thus diffuse "downward." A low dose of impurity atoms that hinder adatom diffusion in the growing layer while staying in this layer as long as possible is capable of introducing such a mobility bias.

All of these suggestions are in fact physically possible through appropriate manipulation of growth parameters. One particularly appealing approach is the deliberate introduction of the right type of impurity—a surfactant. Surfactant-induced layer-by-layer growth has been observed in a variety of systems (*55*). Various mechanisms of surfactant action have been proposed (*48*, *50*, *55*, *56*), none of them related to the classical meaning of "surfactant" as a surface-active agent that reduces the surface free energy. In fact, as used in film growth, surfactants are agents that control kinetics. An ideal surfactant should be: (i) capable of inducing smoother growth; (ii) "immiscible" in the film, so that no or a negligible amount of surfactant atoms are incorporated into the film; and (iii) easily removable at the completion of growth.

Another more traditional way of manipulating growth kinetics is to use vicinal surfaces as templates for growth. If the substrate is miscut at an angle, it contains a collection of steps whose density is determined by the angle of miscut. At properly chosen growth conditions, an atom deposited on a given terrace is always able to reach the steps bounding the terrace and be incorporated there before another atom is deposited in the vicinity; hence, the nucleation rate for islands on the terrace is negligibly small. If any barrier for downward crossing over steps exists, there would be a bias toward incorporation on the ascending steps (at which there exists no barrier for incorporation). A stable "step-flow" growth mode, with equally spaced steps smoothly flowing across the surface, is then established (*53*).

More Complex Growth Situations

In describing atomistic mechanisms of the initial stages of film growth, we have, for the sake of illustration, focused on examples from homoepitaxy, the growth of a material on itself, by vapor deposition of atoms. Although homoepitaxial films are of considerable significance, they form only a small part of industrial thin-film technology. The large prevalence of films is grown on dissimilar substrates, including growth on slightly lattice-mismatched substrates [Stranski-Krastanov growth (*58*)] and growth on very dissimilar substrates [Volmer-Weber growth (*59*)]. These growth modes are principally distinguished by different thermodynamic driving forces, which may introduce new kinetic phenomena or modify the relative importance of the ones we have described.

In addition, methods of deposition extend far beyond the simple deposition of atoms we have used for illustration here. Examples include chemical vapor deposition (CVD) and ion-assisted methods such as sputter deposition. These methods generally introduce additional kinetic processes that influence the rate of growth and quality of the films.

Yet, the atomistic mechanisms described above influence the initial stages of growth without regard to the deposition method or the dissimilarity of film and substrate. For example, in Stanski-Krastanov growth, the stress caused by the mismatch of the lattices of the film and the substrate produces a thermodynamic driving force that modifies structure and morphology. In the submonolayer regime, stress can cause intermixing and alloying through diffusion of some of the deposited atoms into the top layers of the substrate (*60*). For thicker films, a sufficiently high accumulation of strain energy in the system may ultimately cause the strained overlayer to organize into 3D clusters or to create other distributions of defects. A strained overlayer on a vicinal substrate may be energetically unstable against step bunching (*61*). Control of kinetics can be used to suppress intermixing, clustering, and bunching in order to grow heterostructures with atomically flat interfaces, or in the other extreme, to enhance the formation of desirable 3D nanoclusters with well-defined size and spatial distributions (*62*). Impurities added as surfactants, in addition to modifying the magnitudes of kinetic processes, can modify the stress state and thus influence the thermodynamic driving force.

In the limit when the deposited material and the substrate are very dissimilar, the growth becomes rapidly 3D (Volmer-Weber growth), that is, the deposited material does not wet the surface. The kinetic processes that determine the growth are qualitatively similar to the ones discussed here; the differences lie in the thermodynamic driving forces related to minimization of the total free energy. Atoms deposited on the substrate are subject to the same rules except that they now become hetero-mechanisms (for example, atom B diffuses on a substrate of A atoms). Critical nucleus sizes may be different. For atoms on the 3D cluster, the processes are identical to the homoepitaxial ones discussed above, because the 3D cluster is simply a small crystal having terraces, steps, and kinks as in Fig. 1. Thus, a picture very similar to what is laid out above will describe the initial stages of growth in this limit.

Additional kinetic mechanisms can be introduced by the mode of deposition. For example, in CVD (which is used for all three of the classes of film growth mentioned above) a precursor molecule decomposes over a hot substrate, leaving behind the desired atom or atoms while the unwanted molecular fragments of the precursor are removed. The rate of decomposition of this precursor molecule influences the overall rate of film growth. Because the precursor decomposition rate depends on the temperature, the growth temperature and the deposition rate are no longer independent, and thus, the flux and the diffusion rates cannot be independently controlled, as they can in deposition using at-

oms. Molecular fragments adsorbed on the surface may modify the magnitudes of the diffusional or adsorption kinetics (9) but do not qualitatively change the underlying mechanisms.

In ion-assisted deposition methods (the chief example being sputter deposition), the notable feature is the higher energy of the species arriving at the film surface. Primarily, this energy is used to modify film morphology in Volmer-Weber (that is, highly mismatched) film growth and to tailor the stress in such films. Conventional wisdom notwithstanding, sputter deposition can be used for homo- and heteroepitaxy (63) through careful control of deposition parameters, indicating that the same atomistic mechanisms discussed here control the growth.

Film growth is a complex phenomenon. Yet, only a limited number of kinetic mechanisms form the atomistic basis for the initial stages of film growth, no matter what the growth mode or the deposition technique. Here, we have attempted to identify and illustrate such mechanisms.

REFERENCES AND NOTES

1. W. K. Burton, N. Cabrera, F. C. Frank, *Philos. Trans. R. Soc. London Ser. A* **243**, 299 (1951).
2. G. Binnig, H. Rohrer, Ch. Gerber, E. Weibel, *Phys. Rev. Lett*. **49**, 57 (1982).
3. B. S. Swartzentruber, Y.-W. Mo, R. Kariotis, M. G. Lagally, M. B. Webb, *ibid.* **65**, 1913 (1990); X.-S. Wang, J. L. Goldberg, N. C. Bartelt, T. L. Einstein, E. D. Williams, *ibid*., p. 2430.
4. B. Lewis and D. S. Campbell, *J. Vac. Sci. Technol.* **4**, 209 (1967); J. A. Venables, *Philos. Mag*. **27**, 697 (1973).
5. Y.-W. Mo, J. Kleiner, M. B. Webb, M. G. Lagally, *Phys. Rev. Lett.* **66**, 1998 (1991); *Surf. Sci.* **268**, 275 (1992); A. Pimpinelli, J. Villain, D. E. Wolf, *Phys. Rev. Lett.* **69**, 985 (1992).
6. R. M. Tromp, R. J. Hamers, J. E. Demuth, *Phys. Rev. Lett.* **55**, 1303 (1985).
7. J. A. Stroscio, D. T. Pierce, R. A. Dragoset, *ibid.* **70**, 3615 (1993); J. Stroscio and D. Pierce, *Phys. Rev. B* **49**, 8522 (1994); J.-K. Zuo, J. F. Wendelken, H. Dürr, C.-L. Liu, *Phys. Rev. Lett.* **72**, 3064 (1994); H. Dürr, J. F. Wendelken, J.-K. Zuo, *Surf. Sci.* **328**, L527 (1995).
8. H. Brune, H. Röder, C. Boragno, K. Kern, *Phys. Rev. Lett.* **73**, 1955 (1994); M. Bott, M. Hohage, M. Morgenstern, Th. Michely, G. Comsa, *ibid.* **76**, 1304 (1996).
9. J. E. Vasek, Z. Y. Zhang, C. T. Salling, M. G. Lagally, *Phys. Rev. B* **51**, 17207 (1995); P. E. Quesenberry and P. N. First, *ibid*. **54**, 8218 (1996).
10. L. Andersohn, Th. Berke, U. Köhler, B. Voigtländer, *J. Vac. Sci. Technol. A* **14**, 312 (1996); M. Fehrenbacher, J. Spitzmüller, U. Memmert, H. Rauscher, R. J. Behm, *ibid*., p. 1499.
11. J. Villain, A. Pimpinelli, L. H. Tang, D. Wolf, *J. Phys. I* **2**, 2107 (1992).
12. M. C. Bartelt and J. W. Evans, *Phys. Rev. B* **47**, 13891 (1993). G. S. Bales and D. C. Chrzan, *ibid*. **50**, 6057 (1994); C. Ratsch, A. Zangwill, P. Smilauer, D. D. Vvedensky, *Phys. Rev. Lett.* **72**, 3194 (1994); S. Liu, L. Bönig, H. Metiu, *Phys. Rev. B* **52**, 2907 (1995).
13. J. G. Amar and F. Family, *Phys. Rev. Lett.* **74**, 2066 (1995).
14. D. Dijkkamp, E. J. van Loenen, H. B. Elswijk, in *Ordering at Surfaces and Interfaces,* A. Yoshimori, T. Shinjo, H. Watanabe, Eds. (Springer-Verlag, Berlin, 1992), p. 85.
15. N. Kitamura, M. G. Lagally, M. B. Webb, *Phys. Rev. Lett.* **71**, 2082 (1993); Y.-W. Mo, *ibid*., p. 2923.
16. G. Ehrlich and F. G. Hudda, *J. Chem. Phys.* **44**, 1039 (1966).
17. T. T. Tsong, *Phys. Today* **46**, 24 (1993); G. L. Kellogg, *Surf. Sci. Rep.* **21**, 1 (1994).
18. D. W. Pohl and R. Möller, *Rev. Sci. Instrum.* **59**, 840 (1988); B. S. Swartzentruber, *Phys. Rev. Lett.* **76**, 459 (1996).
19. P. J. Feibelman, *Phys. Rev. Lett.* **65**, 729 (1990); G. L. Kellogg and P. J. Feibelman, *ibid.* **64**, 3143 (1990); C. L. Chen and T. T. Tsong, *ibid*., p. 3147.
20. Z. Y. Zhang, Y.-T. Lu, H. Metiu, *Surf. Sci.* **248**, L250 (1991); *ibid*. **255**, L543 (1991); H. Metiu, Y.-T. Lu, Z. Y. Zhang, *Science* **255**, 1088 (1992).
21. Z. Y. Zhang *et al*., *Phys. Rev. Lett.* **74**, 3644 (1995); F. Wu, thesis, University of Wisconsin–Madison (1995).
22. P. Bedrossian, *Phys. Rev. Lett.* **74**, 3648 (1995); R. A. Wolkow, *ibid.*, p. 4448.
23. For a recent review, see Z. Y. Zhang, F. Wu, M. G. Lagally, *Surf. Rev. Lett.* **3**, 1449 (1996).
24. G. Brocks, P. J. Kelly, R. Car, *Surf. Sci.* **269**, 860 (1992); T. Yamasaki, T. Uda, K. Terakura, *Phys. Rev. Lett.* **76**, 2949 (1996); A. P. Smith and H. Jónsson, *ibid*. **77**, 1326 (1996).
25. G. Brocks and P. J. Kelly, *Phys. Rev. Lett.* **76**, 2362 (1996).
26. B. S. Swartzentruber, A. P. Smith, H. Jónsson, *ibid.* **77**, 2518 (1996).
27. R. J. Hamers, U. K. Köhler, J. E. Demuth, *Ultramicroscopy* **31**, 10 (1989); Y.-W. Mo, B. S. Swartzentruber, R. Kariotis, M. B. Webb, M. G. Lagally, *Phys. Rev. Lett.* **63**, 2393 (1989); C. Pearson, M. Krueger, E. Ganz, *ibid.* **76**, 2306 (1996).
28. Y.-W. Mo, R. Kariotis, B. S. Swartzentruber, M. B. Webb, M. G. Lagally, *J. Vac. Sci. Technol. A* **8**, 201 (1990).
29. W. Theis and R. M. Tromp, *Phys. Rev. Lett.* **76**, 2773 (1996).
30. R. Q. Hwang, J. Schröder, C. Günther, R. J. Behm, *ibid.* **67**, 3279 (1991).
31. Th. Michely, M. Hohage, M. Bott, G. Comsa, *ibid.* **70**, 3943 (1993).
32. H. Röder, E. Hahn, H. Brune, J.-P. Bucher, K. Kern, *Nature* **366**, 141 (1993).
33. Z. Y. Zhang, X. Chen, M. G. Lagally, *Phys. Rev. Lett.* **73**, 1829 (1994).
34. Z. Y. Zhang and M. G. Lagally, in preparation.
35. H. Röder, K. Bromann, H. Brune, C. Boragno, K. Kern, *Phys. Rev. Lett.* **74**, 3217 (1995).
36. M. Hohage *et al*., *ibid.* **76**, 2366 (1996).
37. H. Brune *et al*., *Surf. Sci.* **349**, L115 (1996).
38. T. A. Witten and L. M. Sander, *Phys. Rev. Lett.* **47**, 1400 (1981); P. Meakin, *Phys. Rev. A* **27**, 1495 (1983).
39. G. S. Bales and D. C. Chrzan, *Phys. Rev. Lett.* **74,** 4879 (1995).
40. S. Liu, Z. Y. Zhang, G. Comsa, H. Metiu, *ibid.* **71**, 2967 (1993); J. Jacobsen, K. W. Jacobsen, J. K. Nørskov, *Surf. Sci.* **359**, 37 (1996); T.-Y. Fu, Y.-R. Tzeng, T. T. Tsong, *Phys. Rev. B* **54**, 5932 (1996); Ch. Ratsch, P. Ruggerone, M. Scheffler, in *Proceedings of NATO ASI on Surface Diffusion: Atomistic and Collective Processes*, Rhodes, Greece, 26 August to 6 September 1996, M. Tringides, Ed. (Plenum, New York, in press).
41. A. F. Voter, *Phys. Rev. B* **34**, 6819 (1986).
42. J.-M. Wen, S.-L. Chang, J. W. Burnett, J. W. Evans, P. A. Thiel, *Phys. Rev. Lett.* **73**, 2591 (1994); K. Morgenstern, G. Rosenfeld, B. Poelsema, G. Comsa, *ibid.* **74**, 2058 (1995); J. C. Hamilton, M. S. Daw, S. M. Foiles, *ibid*., p. 2760; S. V. Khare, N. C. Bartelt, T. L. Einstein, *ibid.* **75**, 2148 (1995).
43. S. C. Wang and G. Ehrlich, *Surf. Sci.* **239**, 301 (1990).
44. G. L. Kellogg, *Phys. Rev. Lett*. **73**, 1833 (1994).
45. Z.-P. Shi, Z. Y. Zhang, A. K. Swan, J. F. Wendelken, *ibid.* **76**, 4927 (1996).
46. W. Ostwald, *Z. Phys. Chem. (Leipzig)* **34**, 495 (1900).
47. R. L. Schwoebel and E. J. Shipsey, *J. Appl. Phys.* **37**, 3682 (1966).
48. J. Tersoff, A. W. Denier van der Gon, R. M. Tromp, *Phys. Rev. Lett.* **72**, 266 (1994).
49. J. A. Meyer, J. Vrijmoeth, H. A. van der Vegt, E. Vlieg, R. J. Behm, *Phys. Rev. B* **51**, 14790 (1995); K. Bromann, H. Brune, H. Röder, K. Kern, *Phys. Rev. Lett.* **75**, 677 (1995).
50. Z. Y. Zhang and M. G. Lagally, *Phys. Rev. Lett.* **72**, 693 (1994); S. Harris, *Phys. Rev. B* **52**, 16793 (1995).
51. V. A. Markov, O. P. Pchelyakov, L. V. Sokolov, S. I. Stenin, S. Stoyanov, *Surf. Sci.* **250**, 229 (1991); G. Rosenfeld, R. Servaty, C. Teichert, B. Poelsema, G. Comsa, *Phys. Rev. Lett.* **71**, 895 (1993).
52. R. Kunkel, B. Poelsema, L. K. Verheij, G. Comsa, *Phys. Rev. Lett.* **65**, 733 (1990).
53. J. Villain, *J. Phys. I* **1**, 19 (1991).
54. Z. Y. Zhang, J. Detch, H. Metiu, *Phys. Rev. B* **48**, 4952 (1993); H.-J. Ernst, F. Fabre, R. Folkerts, J. Lapujoulade, *Phys. Rev. Lett.* **72**, 112 (1994); M. D. Johnson *et al*., *ibid.*, p. 116; J. E. Van Nostrand, S. J. Chey, M.-A. Hasan, D. G. Cahill, J. E. Greene, *ibid.* **74**, 1127 (1995); J. A. Stroscio, D. T. Pierce, M. D. Stiles, A. Zangwill, L. M. Sander, *ibid.* **75**, 4246 (1995); E. J. Heller and M. G. Lagally, *Appl. Phys. Lett.* **60**, 2675 (1992).
55. D. A. Steigerwald, I. Jacob, W. F. Egelhoff Jr., *Surf. Sci*. **202**, 472 (1988); M. Copel, M. C. Reuter, E. Kaxiras, R. M. Tromp, *Phys. Rev. Lett.* **63**, 632 (1989); S. Esch, M. Hohage, Th. Michely, G. Comsa, *ibid.* **72**, 518 (1994); J. Vrijmoeth, H. A. van der Vegt, J. A. Meyer, E. Vlieg, R. J. Behm, *ibid.*, p. 3843.
56. S. Oppo, V. Fiorentini, M. Scheffler, *Phys. Rev. Lett.* **71**, 2437 (1993); I. Markov, *Phys. Rev. B* **50**, 11271 (1994); D. Kandel and E. Kaxiras, *Phys. Rev. Lett.* **75**, 2742 (1995).
57. J. Jacobsen, K. Jacobsen, P. Stoltze, J. K. Nørskov, *Phys. Rev. Lett.* **74**, 2295 (1996).
58. I. N. Stranski and L. von Krastanov, *Sitzungsber. Akad. Wiss. Wien* **146**, 797 (1938).
59. M. Volmer and A. Weber, *Z. Phys. Chem. (Leipzig)* **119**, 277 (1926).
60. S. Rousset, S. Chiang, D. E. Fowler, D. D. Chambliss, *Phys. Rev. Lett.* **69**, 3200 (1992); F. Liu and M. G. Lagally, *ibid.* **76**, 3156 (1996).
61. J. Tersoff, Y. H. Phang, Z. Y. Zhang, M. G. Lagally, *ibid.* **75**, 2730 (1995).
62. J. Tersoff, C. Teichert, M. G. Lagally, *ibid.* **76**, 1675 (1996).
63. P. Sutter *et al*., *Appl. Phys. Lett.* **65**, 2220 (1994); P. Sutter *et al*., *J. Cryst. Growth* **157**, 172 (1995).

64. We would like to thank F. Wu, X. Chen, Z.-P. Shi, A. K. Swan, M. Hohage, Th. Michely, G. Comsa, H. Metiu, M. B. Webb, and J. F. Wendelken for their contributions and help. Supported by Oak Ridge National Laboratory, which is managed by Lockheed Martin Energy Research Corp. for the Department of Energy under contract DE-AC05-84OR21400, by NSF (grants DMR91-21074 and DMR93-04912), by the Office of Naval Research, and by the Air Force Office of Scientific Research.